Optical Engineering

SPIEDigitalLibrary.org/oe

Megapixel digital InSb detector for midwave infrared imaging

Lior Shkedy
Tuvy Markovitz
Zipi Calahorra
Itay Hirsh
Itay Shtrichman

SPIE

Megapixel digital InSb detector for midwave infrared imaging

Lior Shkedy
Tuvy Markovitz
Zipi Calahorra
Itay Hirsh
Itay Shtrichman
SemiConductor Devices
P.O. Box 2250
Haifa 31021, Israel
E-mail: liorshkedy@scd.co.il

Abstract. Since the late 1990s Semiconductor devices (SCD's) has developed and manufactured a variety of InSb two-dimensional (2D) focal plane arrays (FPAs) that were implemented in many infrared (IR) systems and applications. SCD routinely manufactures both analog and digital InSb FPAs with array formats of 320×256, 480×384, and 640×512 elements, and pitch size in the range 15 to 30 μm. These FPAs are available in many packaging configurations, including fully integrated detector-Dewar-cooler-assembly,, with either closed-cycle Stirling or open-loop Joule–Thomson coolers. In response to a need for very high resolution midwave IR (MWIR) detectors and systems, SCD has developed a large format 2D InSb detector with 1280×1024 elements and pixel size of 15 μm. A digital readout integrated circuit (ROIC) is coupled by flip-chip bonding to the megapixel InSb array. The ROIC is fabricated in CMOS 0.18-μm technology, that enables the small pixel circuitry and relatively low power generation at the focal plane. The digital ROIC has an analog to digital (A/D) converter per-channel and allows for full frame readout at a rate of 100 Hz. Such on-chip A/D conversion eliminates the need for several A/D converters with fairly high power consumption at the system level. The digital readout, together with the InSb detector technology, lead to a wide linear dynamic range and low residual nonuniformity, which is stable over a long period of time following a nonuniformity correction procedure. A special Dewar was designed to withstand harsh environmental conditions while minimizing the contribution to the heat load of the detector. The Dewar together with the low power ROIC, enable a megapixel detector with overall low size, weight, and power with respect to comparable large format detectors. A variety of applications with this detector make use of different cold shields with different F# and spectral filters. In this paper we present actual performance characteristics of the megapixel InSb detector and demonstrate its high manufacturability. [DOI: 10.1117/1.3572163]

Subject terms: infrared fetector; focal plane array; readout integrated circuit; , InSb; detector Dewar cooler; modulation transfer function.

Paper 110103SSPRR received Feb. 1, 2011; revised manuscript received Mar. 7, 2011; accepted for publication Mar. 7, 2011; published online Apr. 00, 2011.

1 Introduction

Semiconductor devices (SCD's) two dimensional (2D) InSb array detector roadmap started in 1997 with the production of 320×256 format and 30 μm pitch detectors, and continued with the larger format of 640×512 elements and pixel sizes of 25, 20, and 15 μm.[1] This roadmap reflects the continuing trend of pixel shrinkage and format growth in infrared 2D arrays, which enables higher resolution and wider field of view (FOV) in infrared (IR) imaging systems. A natural step in the roadmap was the development of Hercules, an InSb detector of 1280×1024 elements and pixel size of 15 μm. Hercules incorporates important technological building blocks that have been developed over the past few years. The first one is a 15 μm InSb pixel, which was introduced in an analog 640×512 array detector in 2007.[2] The second building block of Hercules is the 15-μm digital readout integrated circuit (ROIC) pixel. This new small-pixel design required the use of advanced CMOS technology, 0.18-μm process, which allows for high functionality and relatively low power consumption. A new Dewar technology was required to handle the large mass on the cold finger, resulting from the large size of the focal plane array (FPA). A stiffened Dewar was designed to support the cold finger with rather low contribution to the heat load. The relatively low ROIC power consumption, together with the stiffened Dewar assembly, enabled the integration of the Dewar with a Ricor K548 cryo-cooler, in quite a small overall package size.

In this paper we present the measured electrical and radiometric performance of the Hercules detector. We describe the basic components and technologies which comprise the detector, as well as the detector's parameters and special features.

2 ROIC

Since 2002 SCD has been developing and producing signal processors with analog to digital (A/D) conversion at the focal plane, known as the Sebastian family of ROICs.[3] Three formats of Sebastian ROICs were developed: 320×256, 480×384, and 640×512, all with a 20-μm pixel size and all based on a 0.5-μm CMOS process.[4,5] Sebastian architecture combines a high level of functionality with special

0091-3286/2011/$25.00 © 2011 SPIE

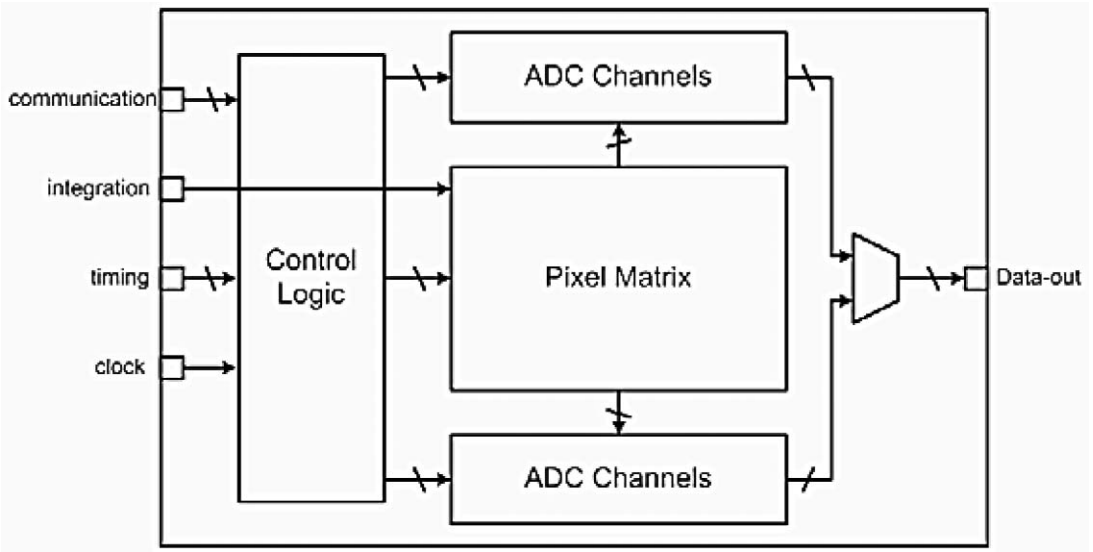

Fig. 1 Block diagram of the Hercules ROIC.

operation modes and excellent performance, especially high linearity and low residual nonuniformity (RNU).[4–6] The main challenge in the new 15 μm pixel design was to maintain the performance level and functionality of Sebastian in half the pixel area. These constraints require the use of a more advanced CMOS process. The CMOS 0.18-μm process by Tower Semiconductor was selected for the new ROIC. A smaller pixel size and a larger format array can affect the following parameters of the ROIC: integration capacitance, power consumption, pixel readout rate, functionality, and readout noise.

The shift to 0.18-μm CMOS process has enabled successful addressing of these parameters due to the following advantages:

- A higher value of capacitance per unit area, which partially compensates for the small area pixel.
- A low operating voltage which reduces power consumption.
- High speed digital circuits.
- A denser layout of devices enables the maintenance of a high level of functionality.
- Using dual threshold voltage (V_{th}) process enables operation of the analog circuits with high voltage and the digital circuits with low voltage.

The first phase of the ROIC design was to update the modeling of the 0.18-μm process for cryogenic operation (77 K). For imager applications the main drawback of an advanced process such as 0.18-μm is noise sources such as 1/f, random telegraph signal (RTS), and various leakage mechanisms, which tend to increase at lower temperatures. Special attention was paid to overcome these noise sources in the design of the Hercules ROIC. The basic architecture of Sebastian was used in the Hercules design, i.e., two rows of A/D channels, each of them consisting of 1280 A/D channels with 15 bit resolution, which read in parallel and convert 2560 pixels simultaneously. A block diagram of the Hercules ROIC is shown in Fig. 1.

In order to support a maximum frame rate of 100 Hz at full window size, the ROIC was designed to operate at a clock rate of 80 MHz. Despite the matrix size and the high data rate of the ROIC, the resultant total power consumption of the ROIC is 80 mW for a 60 Hz and 130 mW for a 100 Hz frame rate at full frame. These relatively low power dissipation values are the result of the low voltage chip operation, which is enabled by the 0.18-μm process. The maximum integration capacitance is 6 Me^- for both integration-then-read (ITR) and integration-while-read (IWR) operation modes. An in-pixel gain was implemented in order to reduce readout noise, which is otherwise dominant by the readout channel. Figure 2 presents a measurement of the squared noise as a function of the signal in the InSb FPA, while the integration time is varied. The linear ratio between the squared noise and the signal indicates shot noise limited detector. These results represent a fine readout process from the ROIC pixel without introduction of any additional noise components. Another key parameter of the ROIC is its linearity. A measurement

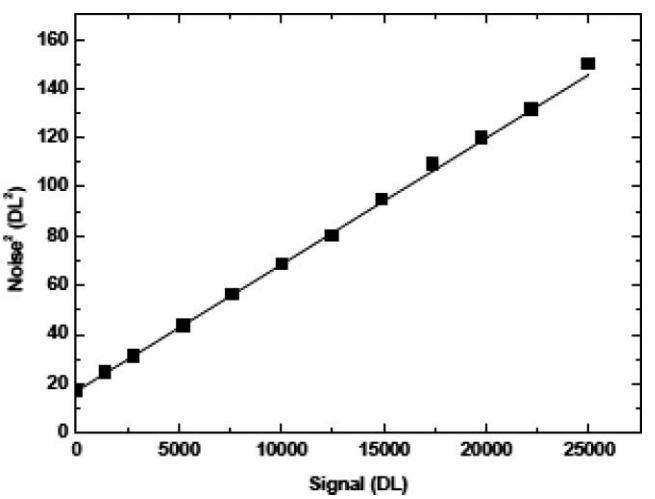

Fig. 2 Square noise as a function of signal in InSb FPA, where the integration time is varied.

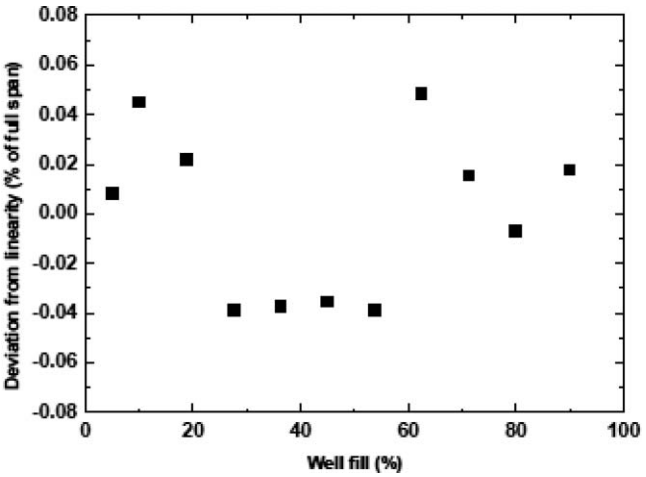

Fig. 3 Deviation from linearity of the Hercules InSb FPA. The well-fill is varied by the integration time.

of the Hercules linearity is presented in Fig. 3. The deviation from linearity is less than 0.06% of the full dynamic range from 5% to 90% capacitor well-fill. This result demonstrates the excellent linearity exhibited by Hercules over almost the full dynamic range.[7] One should note that this level of performance is actually achieved at the system level, since Hercules is a digital ROIC.

3 Electro-Optical Performance

The performance of an array detector is determined by several key properties: the sensitivity is normally defined by the ratio of the temporal noise to the responsivity, known as the noise equivalent temperature difference (NETD), the spatial noise following nonuniformity correction (NUC) procedure (RNU), and the spatial resolution, which is manifested by the inter-pixel cross-talk (XT) or the modulation transfer function (MTF). In this section we present these properties of the Hercules FPA, which are related to both the InSb technology and the ROIC. Table 1 summarizes the main parameters of the Hercules detector.

3.1 *NETD*

Figure 4(a) presents an image of the FPA NETD (per pixel) at 50% well-fill. Due to the low readout noise and low dark current the NETD is background limited (BLIP). As can be seen in the image there are no spatial features in the temporal noise, indicating no additional noise mechanisms aside from the shot noise. In Fig. 4(b) the smooth Gaussian-like histogram of the NETD is shown.

3.2 *RNU*

Figure 3 demonstrates the excellent linearity of the ROIC over almost the entire dynamic range (DR) of the detector. The uniformity of the pixels after linear 2-point NUC is very good as well, due to both the linearity and the high dynamic resistance of the InSb diodes. In order to calculate the correction coefficients, the detector is placed in front of a uniform extended black-body and two measurements at two different black-body temperatures are recorded, keeping the integration time constant. The signal is averaged over a sequence of 32 consecutive frames in order to reduce the effect of the temporal noise on the spatial correction. The two

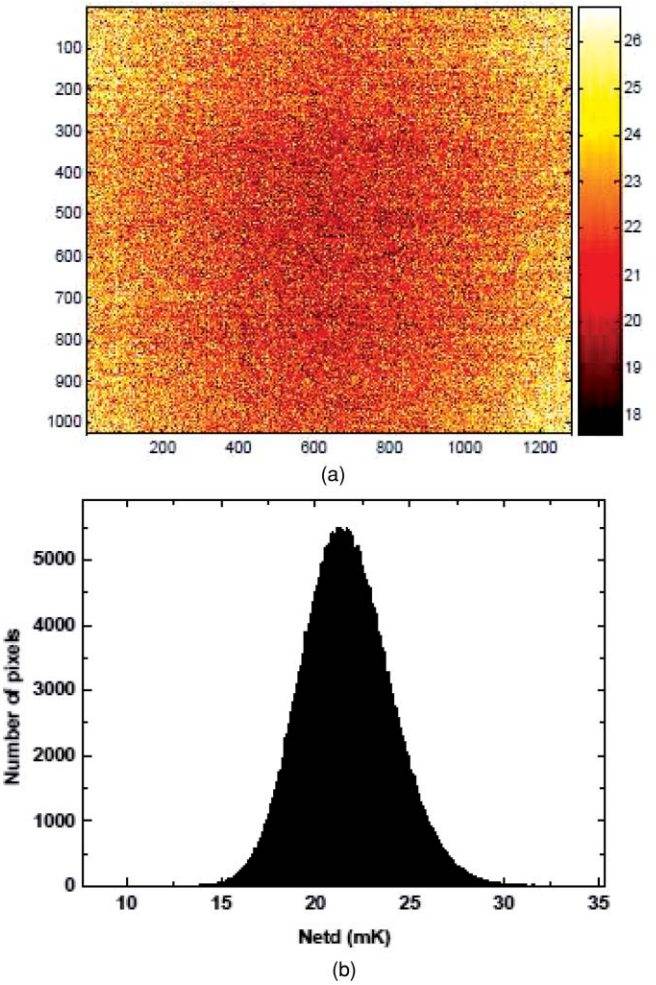

Fig. 4 (a) Hercules NETD image at 50% well-fill, f/4, 77 K. The color scale is in mK. (b) NETD histogram of (a). The average NETD is 22 mK and the std is 2.5 mK.

measured signals are at approximately 20% and 80% well-fill. Using these measurements, the correction coefficients are calculated and used to correct the signal at other black-body temperatures, while keeping the same integration time. The quality of the correction is determined by the spatial standard deviation (std) of all nondefective pixels of the FPA after the correction, when faced in front of a uniform target. This spatial std is the RNU of the detector. In Fig. 5(a) the RNU as a function of well-fill is plotted. As can be seen it is less than 0.03% of the DR over a wide range of well-fills. At the correction points the std is zero by definition. Due to the raw signal nonuniformity caused by the cold shield shadowing of the uniform target ($\cos^4\theta$ effect), the maximal well-fill is around 85% when the first central pixels are saturated. In order to discriminate the high frequency spatial patterns from the low frequency patterns we also calculate the local RNU. This value is a key for determining the ability of the detector to recognize targets from their close environment clutter. The local RNU is the average of the std calculated over the 15×15 neighboring pixels of each pixel. As can be seen it is lower than the global RNU since low frequency patterns are filtered out. In Fig. 5(b) an image of the detector after nonuniformity correction is plotted. As can be seen there is a dominant low spatial frequency residual nonuniformity, which is related to the residual illumination effect, and a

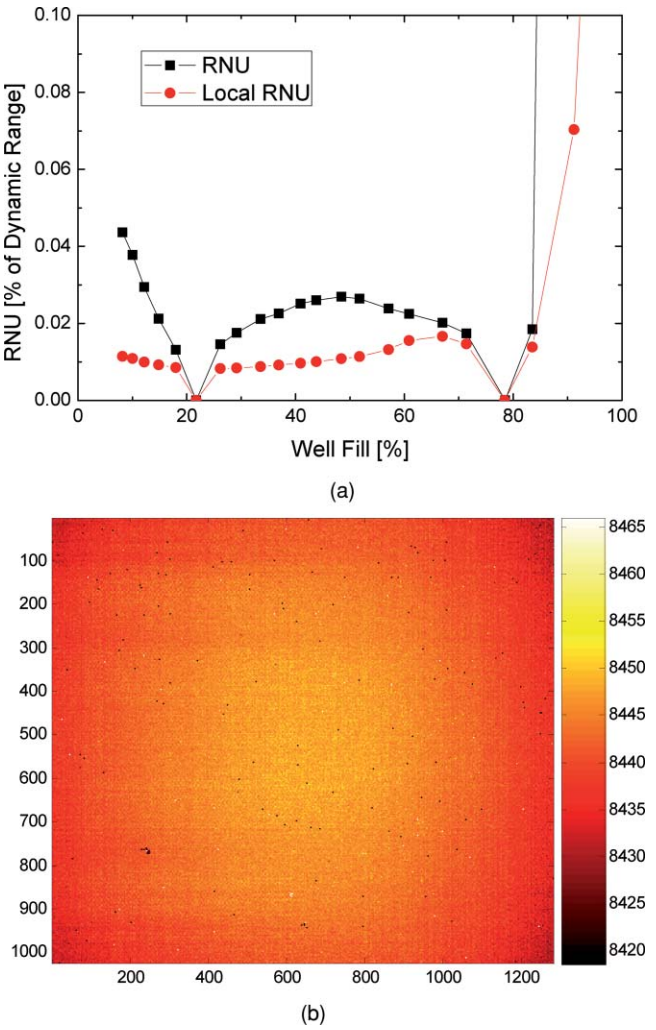

Fig. 5 (a) RNU as a function of well-fill at F/4, 77 K. The signal is varied by the black-body target temperature at constant integration time. (b) An image of a uniform target at 50% well-fill. The color scale is in digital levels. No BPR was applied.

lower random distribution of values which indicate white spatial noise.

Another indicator of the detector quality is its stability over time both for continuous operation as well as for different operations. After cool-down and steady-state operation of the detector, a first set of measurements of variable fluxes at constant integration time was recorded (set-1). The detector was then working continuously for 1, 2, and 4 h, after which the same sequence of measurements was performed (set-2). NUC tables calculated from the first set of measurements (set-1) were applied to the later sets of measurements (set-2), and the RNU was plotted as a function of the well-fill. As seen in Fig. 6, negligible degradation in the RNU was observed. A similar set of measurements was conducted after 5 days of nonoperation. Using the initial NUC coefficient tables, calculated at the first operation (set-1), the RNU was calculated and is also plotted in Fig. 6 versus the well-fill. We find only a slight degradation in the residual uniformity, which indicates that the ROIC is insensitive to power supplies turn-off and turn-on again, and that the InSb diodes do not change their physical properties such as dark current and quantum efficiency (QE) when warmed up and re-cooled again. In Fig. 7

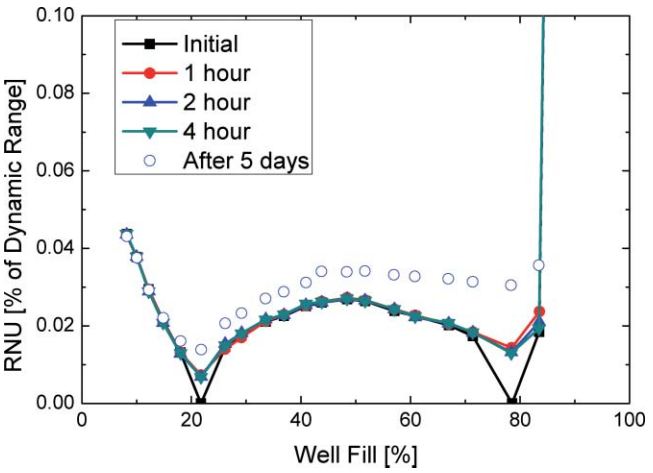

Fig. 6 RNU stability over time.

we present the corrected image of the detector after 5 days of nonoperation using the initial NUC coefficients.

3.3 *MTF*

Ideally, the spatial resolution of the FPA itself (not including system optics diffraction) is determined by the pixel size. However, due to lack of complete separation between the pixels of the array, XT between pixels smears the image. If one pixel in the FPA is illuminated in its center by a "delta function" source, the response will not be only in that pixel but also at some neighboring pixels. The MTF is a measure of the spatial resolution. If the FPA is illuminated by a spatially modulating function of amplitude A_{in}, and the output signal from the FPA at the same spatial frequency has an amplitude A_{out}, then the ratio between the output amplitude and the input amplitude is the MTF at that specific frequency. At zero spatial frequency there is no smearing, so we use that value to normalize the MTF to one. At the Nyquist frequency the MTF is zero since the sampling frequency is at half the frequency of the data.

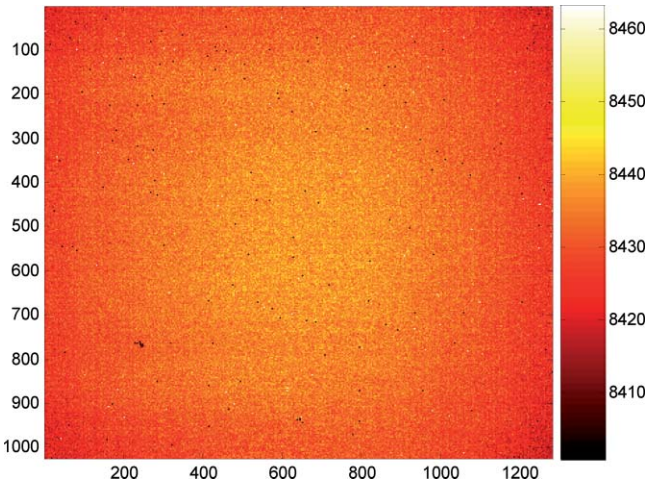

Fig. 7 A corrected image of the detector in front of a uniform black-body after 5 days using the initial NUC coefficient tables. The well-fill is 50% at F/4, 77 K. The color scale is in digital levels. No BPR was applied.

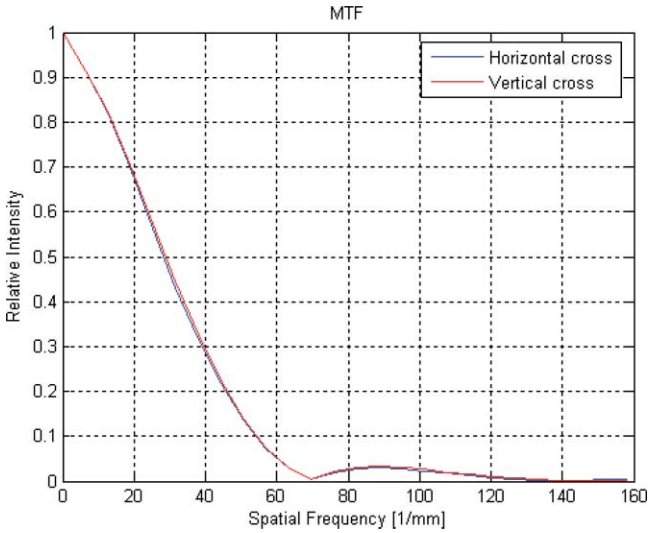

Fig. 8 The MTF (through the pixel center) of a 15μm pixel in InSb FPA.

A detailed description of the FPA MTF measurement is given elsewhere.[8] In short, we measure the MTF of the FPA in an F/1 laboratory Dewar and optics so the measurement would not be limited by optical diffraction of the setup. A collimated narrow band ($\lambda = 4.7 \pm 0.1$ μm) beam from a hot cavity black-body is focused by an F/1 lens on the FPA to produce a spot smaller than the pixel size (approximately 6-μm diam). The spot is first being characterized to give its spatial profile, then using this beam, the pixel and its neighboring 5×5 pixels are scanned at steps of 1 μm. Deconvolution of this measurement with the spot spatial profile gives the point spread function (PSF) of the pixel. The MTF is calculated from the Fourier transform of the PSF, and is presented in Fig. 8. These results also apply to the Hercules FPA.

Since Hercules is a large FPA, maintaining uniform XT over all the FPA is a challenge. We measured the MTF at different points across the Hercules FPA and could not observe any differences, indicating good control over the uniformity of the FPA.

Table 1 Hercules DDCA typical characteristics.

Parameter	Typical value
Well fill capacity	6 Me-
Output digital	15 bit
Integration modes	ITR, IWR, Combined
Maximum frame rate (13 bit)	120 Hz @ 1024×1024
	100 Hz @ 1280×1024
FPA power consumption	90 mW @ 60 Hz
	140 mW @120 Hz
Electrical interface	Camera link
Residual nonuniformity	<0.03% std/full span
NETD with F/5.3 and 50% well-fill	<22 mK
Operability	>99.5%

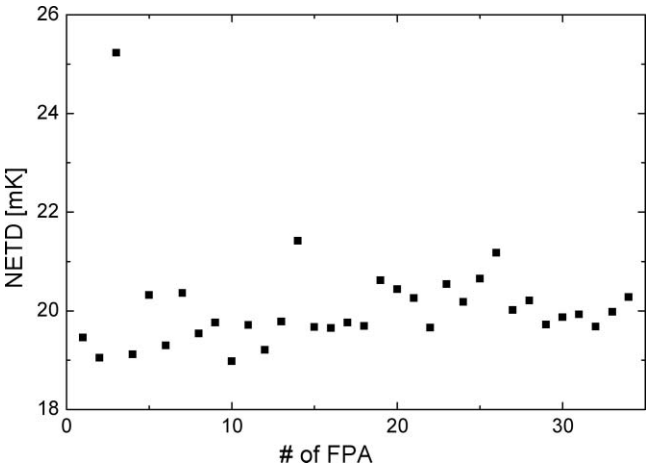

Fig. 9 The average NETD at 50% well fill of 35 Hercules FPAs from the production line. The average NETD is 20 mK and the std is approximately 0.4 mK.

4 FPA Manufacturability

SCD is now able to manufacture Hercules FPAs with good reproducibility and a low number of defective elements. In Figs. 9 and 10 it is shown that the significant parameters that determine the sensitivity, i.e., NETD (average of 20 mK at 50% well-fill) and RNU are not varying considerably from FPA to FPA, and are in accordance with the results demonstrated above for one sample. These values are the averages over an entire FPA. In Fig. 11 it is shown that the number of defective elements is maintained below 0.3% in most FPAs. The defective pixels are found and marked using various algorithms, which are related to responsivity, noise, and other criteria.

5 DDCA Configurations

Despite the large size of the FPA, Hercules is integrated into a standard Dewar, which is based on a rugged Dewar envelope and supporting strings that are connected to the cold finger. The strings are made of material with high stiffness and low

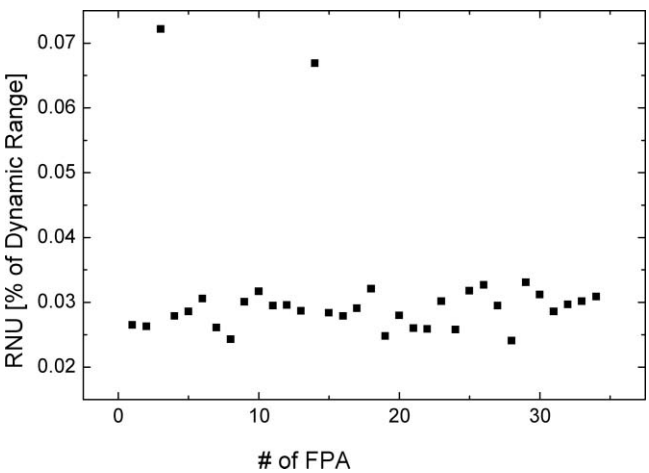

Fig. 10 The measured RNU values in 35 Hercules FPAs from the production line.

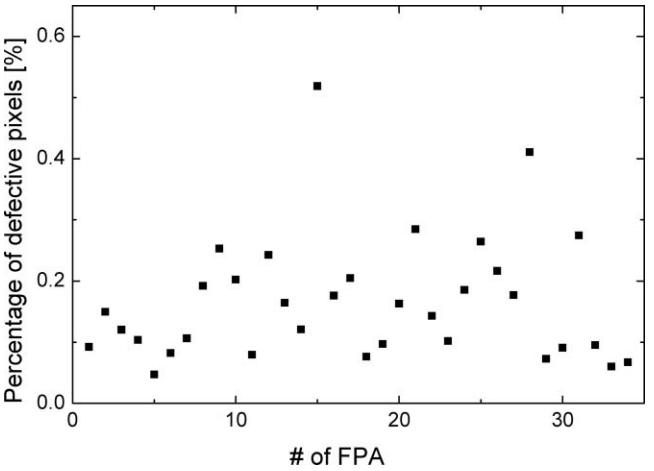

Fig. 11 Percentage of defective pixels in 35 Hercules FPAs from the production line.

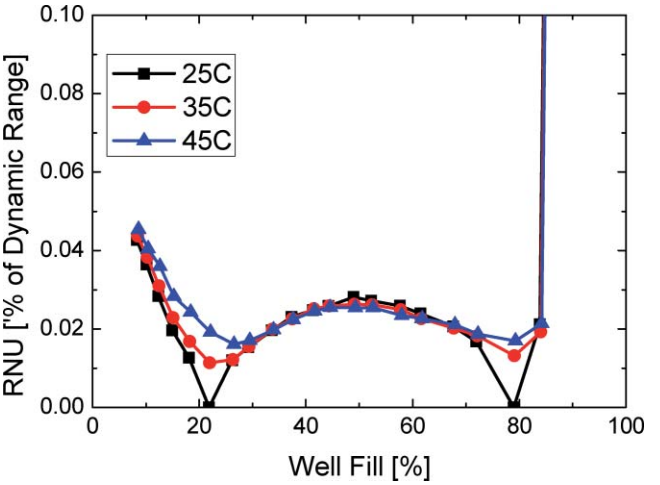

Fig. 13 RNU versus well-fill at different ambient temperatures using the same correction coefficients that were calculated at 25°C ambient temperature.

heat conductivity. The structure and the geometry were optimized to have a high natural frequency combined with low heat conductivity. When the Dewar is assembled with Ricor's K508 half Watt standard cryo-cooler, the natural frequency of the Dewar is about 1500 Hz. This results in a lateral movement of the FPA of less than a third of the pixel size, when subjected to rough vibrations in the frequency range of 5 to 2000 Hz. The resultant heat load of the Dewar enables the integration of the Dewar with either K508 or K548 (cooling power of 0.5 and 0.75 W, respectively), depending on the specific environmental conditions required from the detector, the optical F/#, and the frame rate of operation. In any case the total heat load is less than 0.75 Watt at 71°C, enabling the use of the K548 cooler.

Fig. 12 The Hercules DDCA.

The electronics proximity board that was designed for the Hercules detector is based on the same concept as in the Sebastian detector.[4] The proximity board includes an FPGA, a local oscillator, power supplies and nonvolatile memory components. A single supply of 5 V is input to the proximity board with a noise level of up to 10 mV. The core of the proximity board is a Virtex-5 FPGA, which serves as a buffer between the ROIC and the system, for ROIC operation control, and which controls the data transmission to the system. The FPGA samples the digital data which comes out of the ROIC and performs some basic processing of the data such as pixel remapping and correlated double sampling (CDS). The data is then converted into serial LVDS resulting in a standard medium camera link interface to the system supporting a video data rate of up to 2 Gbit/sec. The system controls the detector with a serial communication command. This concept of a proximity board with a single power supply and camera link interface to the system enables fast and easy integration of the detector into the system. A picture of the DDCA with K508 cooler is shown in Fig. 12.

The results in Fig. 6 show the stability of the FPA (InSb and ROIC) and are also related to the proximity electronics ability to supply accurate and stable power supplies and the ability of the Dewar to withstand environmental changes without affecting the FPA. In order to withstand environmental temperature changes a careful design of the cold radiation shield is needed using ray tracing simulation. The simulation enables the design of a cold shield that absorbs almost all radiation that is emitted by the Dewar and allows only radiation that comes from the desired FOV. Reflections of radiation not in the FOV into the cold shield are absorbed. The test of this characteristic was performed in an environmental chamber. The detector was cooled down and operated at ambient temperature of 25°C. A first set of measurements was conducted

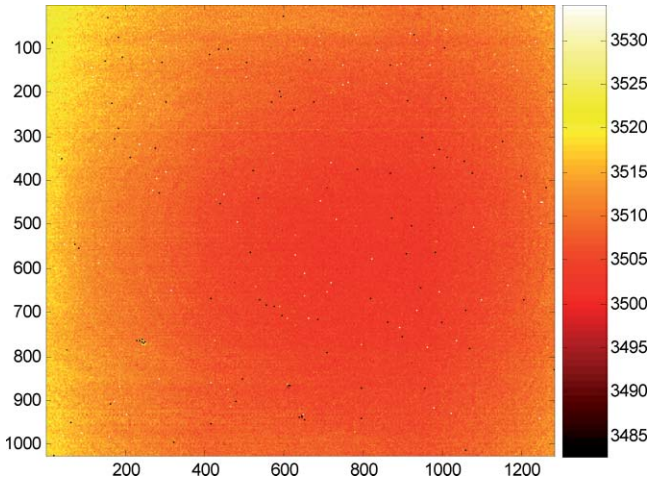

Fig. 14 A corrected image of the detector at ambient temperature of 45°C using correction coefficients calculated at ambient temperature of 25°C. The color scale is in digital levels. No BPR was applied.

Fig. 15 An image obtained using Hercules DDCA from 8 km range. Courtesy of VISIONMAP LTD.

from which the NUC coefficients were calculated. Following, the temperature in the chamber was varied. At each environmental temperature, a similar set of measurements was conducted, while keeping the same integration time. NUC was then performed using coefficients calculated from the first set of measurements and the RNU was plotted versus the well-fill in Fig. 13. We find that although the ambient temperature was increased by 20°C, the RNU degraded only slightly near the correction points. We relate this minor RNU degradation to the IR radiation emission from the window, which is in the FOV. Only negligible stray light from other parts of the Dewar was detected. Figure 14 shows the image at ambient temperature of 45°C following the NUC as explained above. It is apparent that the residual pattern has low spatial frequency, which supports the conclusion that the cause of the minor RNU degradation is stray light from the Dewar only, and not from electrical components induced drifts.

6 Summary

In this paper we present the characteristics of Hercules, a high resolution 1280×1024 element array detector with a 15-μm pixel, based on SCD's well established InSb technology. The development of this detector incorporated several technological building blocks. The Hercules ROIC is SCD's first 0.18-μm CMOS-based product. The 0.18-μm technology has demonstrated its advantages for a large array with a small pixel size. The high functionality, low power consumption, and high pixel capacitance that normally characterize arrays with large pixels has been maintained in this FPA. Another building block that has been used is the 15-μm InSb pixel, which was demonstrated previously in the smaller format Pelican analog detector. In order to handle the large FPA, the Dewar is stiffened using supporting strings, which do not make a significant contribution to the total heat load. The advantages of a digital ROIC are very clear in large format detectors, such as Hercules, where no external A/D converters are needed and the overall system power consumption is much lower with respect to equivalent analog detector.

The Hercules detector demonstrates excellent radiometric characteristics including a high level of linearity and low RNU, from 5 to 90% well-fill capacity. The RNU is maintained low during continuous operation of few hours. Even after warm up, electronic shut down, re-cooling and power-up of the detector, one can use the same NUC coefficient tables from the original calibration. Moreover, due to careful Dewar and proximity electronic design, low RNU is maintained over a large range of ambient temperature changes without the need for updating the NUC coefficients.

The relatively low level of Dewar heat load and ROIC power consumption in the Hercules detector enables the use of standard Stirling cryo-coolers such as Ricor's K508 and K548, or Joule–Thompson coolers for fast cool-down applications. Finally, Fig. 15 shows the superb image quality that can be obtained with the Hercules detector.

Lately, we leveraged the successful Hercules ROIC to introduce a smaller format, 640×512 array, named Pelican-D. We use the same 15-μm InSb and ROIC pixel as in Hercules with the appropriate adaptation for the smaller format. The Pelican-D is mainly characterized by a low level of power consumption (∼35 mW at 60 Hz), enhanced sensitivity, and high frame rate (up to 300 Hz at full VGA format). The Pelican-D FPA fits our standard mid-format Dewars, which are integrated with Ricor's K508, K561, and K562 cryo-coolers, depending on the exact environmental conditions. As such, the Pelican-D supports a large variety of applications such as Hand-held, missile warning systems (MWS), missile seekers, etc.

References

1. O. Nesher and P. Klipstein, "High performance IR detectors at SCD present and future," *Proceedings of SPIE Infrared Photoelectronics*, **5957**, The international society for optical engineering, pp. 0S1-OS12 (2005).
2. J. Oiknine Schlesinger, Z. Calahorra, E. Uri, O. Shick, T. Fishman, I. Shtrichman, E. Sinbar, V. Nahum, E. Kahanov, B. Shlomovich, S. Hasson, N. Fishler, D. Chen, and T. Markovitz, "Pelican – SCD's 640×512/15 μm pitch InSb detector," *Proceedings of SPIE Infrared Technology and Applications XXXIII Conference*, **6542**, pp. 654231–1–8 (2007).
3. S. Elkind, A. Adin, I. Nevo, and A. B. Marhasev, "Focal plane processor with a digital video output for InSb detectors," *Proceedings of SPIE Infrared Technology and Applications XXVIII Conference*, **4820**, pp. 751–757 (2002).

4. O. Nesher, S. Elkind, A. Adin, I. Nevo, A. B. Yaakov, S. Raichshtain, A. B. Marhasev, A. Magner, M. Katz, T. Markovitz , D. Chen, M. Kenan,A. Ganany, J. Oiknine Schlesinger, and Z. Calahorra, "A Digital Cooled InSb Detector for IR Detection," *Proceedings of SPIE Infrared Technology and Applications XXIX Conference*, **5074**, pp. 120 (2003).
5. O. Nesher, S. Elkind, I. Nevo, T. Markovitz, A. Ganany, A. B. Marhashev, and M. Ben-Ezra, "480×384 Element InSb Detector with Digital Processor", *Proceedings of SPIE Infrared Technology and Applications XXX Conference* **5406**, pp. 214–221 (2004).
6. O. Nesher, S. Elkind, G. Francis, and M. Kenan, "SCD solutions for Missile Warning System Applications," *Proceedings of SPIE Infrared Technology and Applications XXXII* **6206**, pp. 62061Z1–11 (2006).
7. O. Nesher, I. Pivnik, E. Ilan, Z. Calahorra, A. Koifman, I. Vaserman, J. Oiknie Schlesinger, R. Gazit, and I. Hirsh, "High resolution 1280×1024, 15 μm pitch compact InSb IR detector with on-chip ADC," *Proceedings of SPIE,,Infrared Technology and Applications XXXV Conference* **7298**, pp. 72983K-1–9 (2009).
8. I. Shtrichman, T. Fishman, U. Mizrahi, V. Nahum, Z. Calahorra, and Y. Aron, "Spatial resolution of SCD's InSb 2D detector arrays," *Proceedings of SPIE, Infrared Technology and Applications XXXIII Conference*, **6542**, pp. 65423M-1–11 (2007).

Biographies and photographs of the authors not available.